Ambient Seismic Vibrations in Seismology and Earthquake Engineering

Francisco J. Sánchez-Sesma
Instituto de Ingeniería, Universidad Nacional Autónoma de México;
Coyoacán 04510, México DF, Mexico. sesma@unam.mx

ABSTRACT

The last decade witnessed the specular emergence of **ambient seismic noise** as a powerful tool for imaging Earth structure at many different scales. Applications are emerging for sundry data sets with better understanding for a wide range of applications in **Seismology** including time-dependent imaging, underwater acoustics, helioseismology, and structural health monitoring, to cite only a few. These advances powered also significant applications in **Earthquake Engineering** as well. Besides noise-based imaging, innovative applications arise to establish dominant periods of sites and inverting the soil structure in order to compute seismic response.

This communication aims to review this wide subject. The author chooses as a conducting thread the energy, specifically the Principle of Equipartition of Energy and its implications in dynamic elasticity. The point of view is rather personal and links the multiple scattering with the idea of diffuse fields in which the energy equilibrate to fulfill the conditions predicted by the theory. The experimental verification of these predictions is discussed. It is then proposed that a random set of plane waves that fulfill the equipartition principle allows to retrieve from correlations the Green's function and allows defining a diffuse field. A correlation type representation theorem is used as a tool to derive useful equations. The use of emerging applications are discussed: The computation of Green's functions using equipartitioned cocktails of plane waves and the tomography of an alluvial valley using earthquake data collected along the years. The auto-correlations are related to directional energy densities and this leads to the deterministic partitions of energy and the interpretation of the noise H/V spectral ratio in terms of the Green's functions. This allows to deal with layered media and consider inversion from surface data and at depth. The effects of lateral heterogeneity can be studied from the same point of view.

INTRODUCTION

The extraction of deterministic information about the Earth structure from long ambient-noise time series opens new opportunities for seismologists. Correlations of ambient seismic vibrations are effectively and widely used to reconstruct impulse responses between two passive receivers as if a source was placed at one of them. This opens the opportunity for imaging without a source; this is passive imaging.

The last decade witnessed the specular emergence of ambient seismic noise as a powerful tool for imaging Earth structure at many different scales. All this lead to improvement of the methods that utilize ambient noise. They are now applied to more data sets with better theoretical understanding. They are useful for a wide range of applications in Seismology including time-dependent imaging, and imaging of sundry physical processes like helioseismology, underwater acoustics, and structural health monitoring, to cite only a few.

These advances powered also significant applications in Earthquake Engineering as well. In addition to improved performance of noise-based imaging, there are innovative applications to establish dominant periods of sites and inverting the shallow soil structure.

The correlation approach is linked with early seismological developments in this century but the roots are in earlier pioneering works, such as those of Aki (1957) and Clearbout (1968). The new field has grown rapidly. There are comprehensive reviews (e.g. Campillo 2006, Larose et al. 2006, Gouédard et al. 2008, Courtland 2008, Wapenaar et al. 2010a 2010b, Snieder and Larose 2013, Campillo 2014). The book by Sato et al. (2012) gives a full account.

This communication is focused on ambient seismic noise in seismology and earthquake engineering. It explores the phenomenological emergence of diffuse fields from multiple scattering and delves into the properties of equipartition of energy that lead to the Green's function retrieval from average correlations within diffuse fields. The concept of energy densities and its relations with average autocorrelations is explained and their directional character is stated. We pointed out the two faces of equipartition. This means, the equipartition of energy can be considered in terms of states and modes but also in terms of degrees of freedom. This opens the connection with deterministic studies of energy partition of energy due to loads and lead to the interpretation of noise horizontal-to-vertical spectral ratios NHVSR in terms of diffuse field concepts. Recent developments include H/V at depth and considering lateral heterogeneity and a fast algorithm to compute H/V that uses Cauchy´s residue theory that allows for inversion of soil profile with only one station. Emerging applications of the theory allows to model H/V under lateral irregularity.

GREEN´S FUNCTION RETRIEVAL

In his pioneering studies Aki (1957) insisted that seismic noise and the coda of earthquakes may contain valuable information of the surrounding media. Aki's long term plan ranged from single and multiple scattering descriptions to radiative transfer ideas aimed to explain coda envelopes. A comprehensive account can be found in Sato and Fehler (1998) and Sato et al (2012).

Equipartition means that in the phase space the available energy is equally distributed, with fixed average amounts, among all the possible states. This simple yet powerful concept is one of the building blocks of modern thermodynamics, and it has also been put forward for multiple scattered waves and explicitly for elastic waves. It was first discussed by Weaver (1982) for elastic waves in a solid body, giving the proportions of energy carried by P and S waves. Weaver (1982) extended Rayleigh's elegant mode-counting argument. On the other hand Ryzhik *et al.* (1996) formally established the transport equation of elastic waves and the associated diffusion approximation. They pointed out that in such diffusive regimes the *P* to *S* energy ratio equilibrates in a universal way independent of details of the multiple scattering. The same solution was obtained by Snieder (2002) who used a probabilistic ball-counting algorithm. Such energy ratio is $E_S/E_P = 2\alpha^3/\beta^3 = R^3$ where E_S and E_P are the *S* and *P* waves spatial energy densities, and α and β are the propagation velocities of P and S waves, respectively. In real materials the multiple scattering that takes place generates an

interesting fact. Although in the micro-scale the field equations remain the same (Newton and Hooke's laws, thus Navier's equations) intensities, like other averages, they follow diffusive processes and these averages satisfy diffusion-like equations (e.g., heat equation).

Evidence of the transition toward equipartition has been observed in real data (Hennino *et al.*, 2001; Shapiro *et al.*, 2000) from the observation of the stabilization of the *P* to *S* energies ratio in the coda at a value compatible with the theory. In fact, coda waves are natural candidates to undergo equipartition. This is attested by the stabilization of the energies ratio. Coda waves continue ringing for a duration many times longer than the source–site travel time, and this clearly suggests multi-paths. The exponential decay of coda waves, characterized by the coda *Q* that, although frequency dependent, is a regional constant, is independent of magnitude and source depth (Aki and Chouet, 1975) and indicates that coda waves sample the Earth uniformly around the recording station. Equipartition is expected to arise naturally in the diffusive regime. The energy ratio stabilization appears before the complete isotropy of the field but indicates that the diffusion can be used as a good approximation (Paul *et al.*, 2005).

Sánchez-Sesma and Campillo (2006) considered the canonical problem of a uniform random distribution of plane waves within a homogeneous elastic medium. The cross correlation of the fields produced at two points by generic plane waves is computed and azimuthally averaged. They used polar and spherical coordinates for the 2D and 3D cases, respectively, and found that the Fourier transform of the average of the cross correlation of motion between two points is proportional to the imaginary part of the tensor Green's function between these points, provided the energy ratio E_S/E_P is precisely the one that arises from equipartition. These results show that, for an elastic medium, equipartition is a necessary condition to retrieve the Green's function from correlations of the isotropic elastic field.

The case of an elastic inclusion was also discussed by Sánchez Sesma *et al.* (2006). These results were generalized by Sánchez Sesma *et al.* (2008) using Somigliana's representation theorem as departing identity to write down a correlation type representation theorem:

$$2\mathrm{i}\,\mathrm{Im}\left[G_{ij}(\mathbf{x}_A,\mathbf{x}_B)\right]=-\oint\left\{G_{il}(\mathbf{x}_A,\mathbf{x})T^*_{lj}(\mathbf{x},\mathbf{x}_B)-G^*_{jl}(\mathbf{x}_B,\mathbf{x})T_{li}(\mathbf{x},\mathbf{x}_A)\right\}dS\,. \qquad (1)$$

Here $G_{ij}(\mathbf{x}_A,\mathbf{x}_B)$ = Green's function in frequency domain which is the displacement at $\mathbf{x}_A$ in direction *i* produced by a unit harmonic point force acting at $\mathbf{x}_B$ in direction *j*. $T_{ij}(\mathbf{x}_A,\mathbf{x}_B)$ = traction Green's function which is the traction at $\mathbf{x}_A$ in direction *i* in a face with specified normal $\mathbf{n}(\mathbf{x}_A)$ produced by a unit harmonic point force acting at $\mathbf{x}_B$ in direction *j*. The asterix means complex conjugate. The factor $\exp(i\omega t)$ is omitted here and hereafter. From Eq. 1 and assuming a closed spherical contour and asymptotic expressions for Green's tensors Sánchez-Sesma et al (2008) obtained:

$$\left\langle u_i(\mathbf{x_A},\omega)u^*_j(\mathbf{x_B},\omega)\right\rangle=-2\pi\,E_S k^{-3}\,\mathrm{Im}\left[G_{ij}(\mathbf{x_A},\mathbf{x_B},\omega)\right], \qquad (2)$$

where the brackets mean azimuthal average and E_s the average energy density of the shear waves within the isotropic background field. It is from this relationship that one can talk of Green function retrieval from cross correlations.

In both the homogeneous and inhomogeneous cases, the equipartition of the background field is a necessary and sufficient condition to retrieve the *exact* Green's function from correlations.

ENERGY DENSITIES

Consider Eq. 2 when source and receiver coincide that is to say $\mathbf{x}_A = \mathbf{x}_B = \mathbf{x}$. In that case the left hand side is just the spectral density or the auto-correlation. This is a finite quantity. One can write for the directional energy density in direction 1 by means of:

$$E_1(\mathbf{x},\omega) = \rho\omega^2 \left\langle u_1(\mathbf{x},\omega) u_1^*(\mathbf{x},\omega) \right\rangle = -2\pi\mu E_S k^{-1} \mathrm{Im}\left[G_{11}(\mathbf{x},\mathbf{x},\omega)\right]. \tag{3}$$

The right hand side is also finite because the singularity of Green's function is restricted to the real part, the imaginary part is healthy and represents the radiated energy into the medium by the unit harmonic load. From the classical Stokes' (1849) solution it is possible to write

$$\mathrm{Im}\left[G_{11}(\mathbf{x},\mathbf{x},\omega)\right] = -\frac{\omega}{12\pi\rho}\left(\frac{1}{\alpha^3}+\frac{2}{\beta^3}\right). \tag{4}$$

Thus, from Eqs. 3 and 4 we have:

$$E_1(\mathbf{x},\omega) = 2\pi\mu E_S k^{-1} \frac{\omega}{12\pi\rho}\left(\frac{1}{\alpha^3}+\frac{2}{\beta^3}\right) = \frac{E_S\beta^3}{6\alpha^3}\left(1+2R^3\right) = \frac{E_P}{3}\left(1+2R^3\right) = \frac{E_P}{3}+\frac{E_S}{3}. \tag{5}$$

Writing energy density as ξ one can write $\xi_P + \xi_{SH} + \xi_{SV} = \xi$ and $\xi_S / \xi_P = 2(\alpha/\beta)^3 = 2R^2$. Let us follow Weaver (1985) and write:

$$\begin{aligned}
\xi_P &= \frac{1}{1+2R^3}\xi \\
\xi_{SH} &= \frac{R^3}{1+2R^3}\xi \\
\xi_{SV} &= \frac{R^3}{1+2R^3}\xi
\end{aligned} \tag{6}$$

It is instructive to regard the partitions in terms of degrees of freedom. After Sánchez-Sesma and Campillo (2006) one can write:

$$\begin{aligned}
\xi_1 &= \frac{1}{3}\xi_P + \frac{1}{6}\xi_{SV} + \frac{1}{2}\xi_{SH} = \frac{1}{3}\xi \\
\xi_2 &= \frac{1}{3}\xi_P + \frac{1}{6}\xi_{SV} + \frac{1}{2}\xi_{SH} = \frac{1}{3}\xi \\
\xi_3 &= \frac{1}{3}\xi_P + \frac{2}{3}\xi_{SV} \qquad\qquad = \frac{1}{3}\xi
\end{aligned} \tag{7}$$

Where ξ_i is the energy density in direction i. Clearly $\xi_1 + \xi_2 + \xi_3 = \xi$ which shows that energy can be also described using degrees of freedom. In a half-space in addition of P and S waves an extra state has to be considered: Rayleigh waves. According to Weaver (1985) and Perton (2009) we have

$$\begin{aligned}
\xi_P &= \frac{1}{1+2R^3}\xi \\
\xi_S &= \frac{2R^3}{1+2R^3}\xi \\
\xi_R &= \frac{\pi\beta}{\omega}\left(\frac{\beta}{c_R}\right)^2 \frac{R^3}{1+2R^3}\xi
\end{aligned} \tag{8}$$

These ideas have been extended by Perton et al (2009) to compute energy densities against depth in an elastic half-space. These authors computed the energy densities for incidence of an equipartitioned set of elastic waves. Fig. 1 depicts the results and shows two ways in which equipartition may occur: the energy densities can be described in terms of states and degrees of freedom. As one may suspect the total energy density is the same. This extends the elementary results for the full space to the half space with free surface and firmly establish the concept of directional energy density.

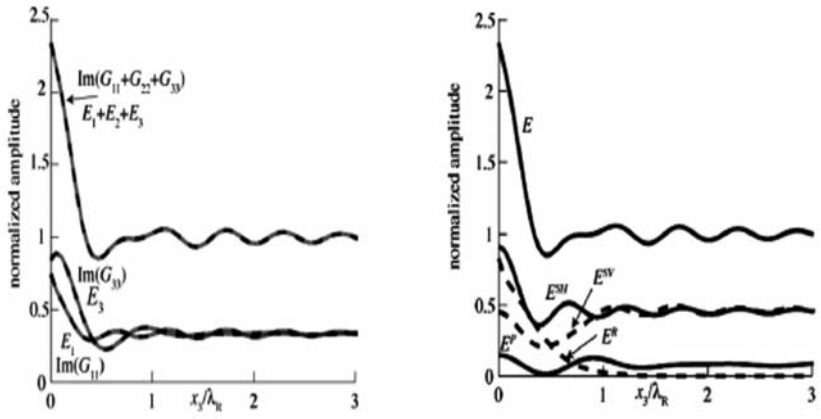

Figure 1, Left: Energy densities for the three orthogonal directions. Directional energies E_1, E_2 and E_3 with black discontinuous line. Right: Energy densities for incoming P, SV, SH, and R waves. Both panels are against normalized depth x_3/λ_R, where λ_R = wavelength of Rayleigh waves. In left panel the gray continuous lines come from the imaginary part of the Green function components *at*

the source, computed from the integral representation. In the right panel, the cases of SV and Rayleigh waves are drawn with discontinuous lines (after Perton *et al*., 2009). Amplitudes are normalized in terms of the energy density in deep space.

EXPERIMENTAL VALIDATION

These ideas have been tested in the field with a careful experiment in Chilpancingo, (Mexico). A small aperture array of four stations was deployed and 11 events were recorded (Campillo et al. 1999, Shapiro et al. 2000). The stations were located in the corners of a square with side of 50m thus spatial derivatives could be computed and the field could be separated into P and S waves. Fig. 2 shows some results four one of the recorded events (Hennino, 2001). It was found a fairly constant ratio of energies due to S and P waves. This is the first verification of equipartition in a seismic wave field.

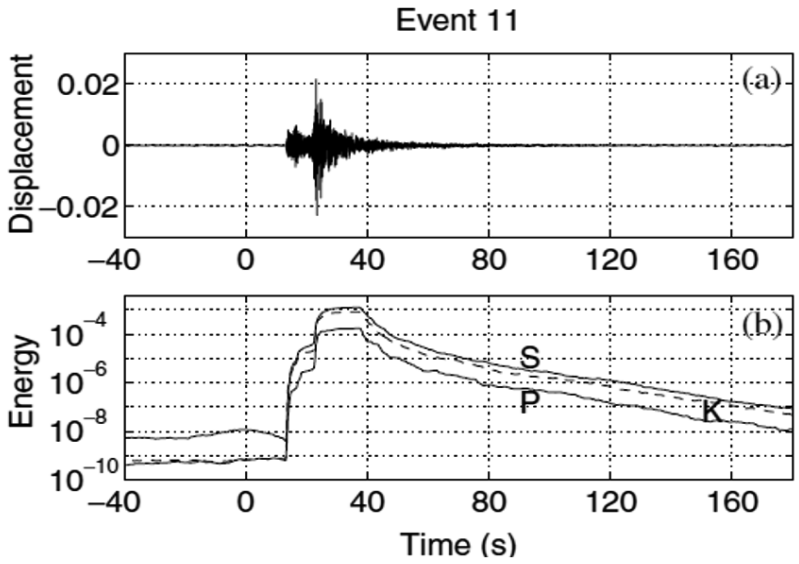

Figure 2. Observed seismogram at Chilpancingo (Mexico), bandpassed between 1 and 3 Hz, for the event 11 at an epicentral distance of 35 km from the array and a magnitude of 4.3. (a) Linear plot of the band passed displacement measured as a function of time. (b) Semi logarithmic plot of the energy density. A distinction is made between kinetic energy (*K*, dashed line), shear energy (*S*), and compressional energy (*P*). (After Hennino et al., 2001).

PARTITION OF ENERGY FOR SURFACE LOADS

The energy partitions among elastic waves due to dynamic normal surface load in a semi-infinite elastic solid with Poisson ratio of 0.25 was studied by Miller and Pursey (1955). For a tangential load the research is little known. It comes out that such partitions for both normal and tangential loads were computed independently by Weaver (1985) versus Poisson ratio ($0 \leq \nu \leq 0.5$), using diffuse-field concepts of room acoustics within the context of ultrasonic measurements.

The connection with the surface load point was not explicit, which partially explains why these results did not reach the seismological and engineering literature. The characteristics of the elastic radiation of these two cases are quite different. For a normal load, about 2/3 of the energy leaves the loaded point as Rayleigh surface waves. On the other hand, the tangential load induces a similar amount in the form of body shear waves. The energies injected into the elastic half-space by concentrated normal and tangential harmonic surface loads are proportional to the imaginary part of the corresponding components of the Green's tensor when both source and receiver coincide.

The relationship between the Green's function and average correlations of motions within a diffuse field is now clearly established. This is worth emphasizing because this in turn implies that we can measure them in the field (i.e., horizontal-to-vertical H/V spectral ratios related to energy partitions) if the seismic noise is diffuse.

Sánchez-Sesma *et al*. (2011a) identified the connection under a new perspective. They pointed out that average measurements of ambient vibrations may reveal intrinsic properties of systems. In fact, calculations based on the diffuse-fields concepts allow to deterministically obtain the energy partitions of the energy injected on the elastic half-space by surface loads. These canonical results can be of interest in several fields.

GREEN'S FUNCTION COMPUTATION FROM CORRELATIONS

In the framework of the partition of the energy injected into a half-space by surface loads, it was made explicit the connection between the elastic Green´s function and the diffuse field theory (Sánchez-Sesma *et al.* 2011a). One interesting application is the computation of Green's function from correlations. The half-space is a very useful case as it allows to explore the computation of Green's functions at the half-space from a set of equipartitioned elastic plane waves including Rayleigh waves. This approach allows for faster computation as compared with DWN.

The analytical solution for the dynamic response of an elastic half-space for a normal point load at the free surface is due to Lamb (1904). The corresponding solution for a tangential load was obtained by Chao (1960). These authors expressed their solutions using integral representations in the radial wavenumber domain. It is possible to express in the same fashion the field produced by an arbitrary load at any depth of half-space. Computations are usually made using the discrete wave number (DWN) formalism and Fourier analysis allows passing to time domain. From Eq. 2 one can write

$$\mathrm{Im}\left[G_{ij}(\mathbf{x_A},\mathbf{x_B},\omega)\right] = -\frac{\omega}{2\pi\rho\beta^3 S^2}\left\langle u_i(\mathbf{x_A},\omega)u_j^*(\mathbf{x_B},\omega)\right\rangle . \qquad (9)$$

Considering the weights given in Eq. 8 and illuminating the half space with plane P, SV, SH and Rayleigh waves as indicated in the Fig 3. For homogeneous plane waves the free surface produces the corresponding reflections.

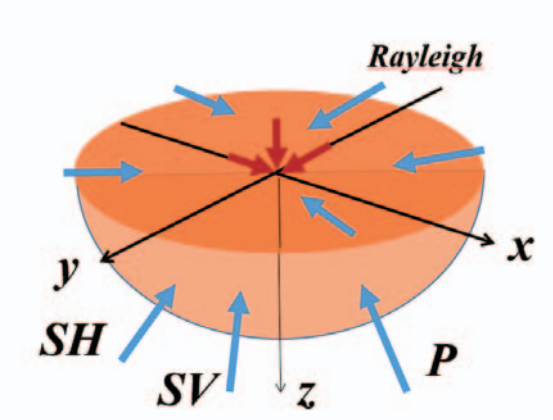

Figure 3. Illumination of half-space with incoming P. SV. SH and Rayleigh waves.

The computation of Green function for a surface unit vertical load is precisely Lamb's (1904) problem. In frequency domain this solution for radial and vertical displacements are formally given by

$$G_{r3}(r,z,\omega)=\frac{1}{2\pi\mu}\int_0^\infty \frac{(k^2-\nu^2)e^{-i\gamma z}+2\gamma\nu\, e^{-i\nu z}}{(k^2-\nu^2)^2+2\gamma\nu k^2}\,k^2 J_1(kr)dk\,,\ \text{and} \tag{10}$$

$$G_{33}(r,z,\omega)=\frac{i}{2\pi\mu}\int_0^\infty \frac{(k^2-\nu^2)e^{-i\gamma z}-2k^2\, e^{-i\nu z}}{(k^2-\nu^2)^2+2\gamma\nu k^2}\,\gamma k J_0(kr)dk\,, \tag{11}$$

Respectively. Here $k=$ radial wavenumber, $J_n(\bullet)=$ Bessel function of first kind and order n,
$\nu=\sqrt{\omega^2/\beta^2-k^2}$ with $\mathrm{Im}(\nu)\le 0$ and $\gamma=\sqrt{\omega^2/\alpha^2-k^2}$ with $\mathrm{Im}(\gamma)\le 0$ are vertical wavenumbers. Results are depicted in Fig. 4 for source and receiver at the surface. Agreement is excellent.

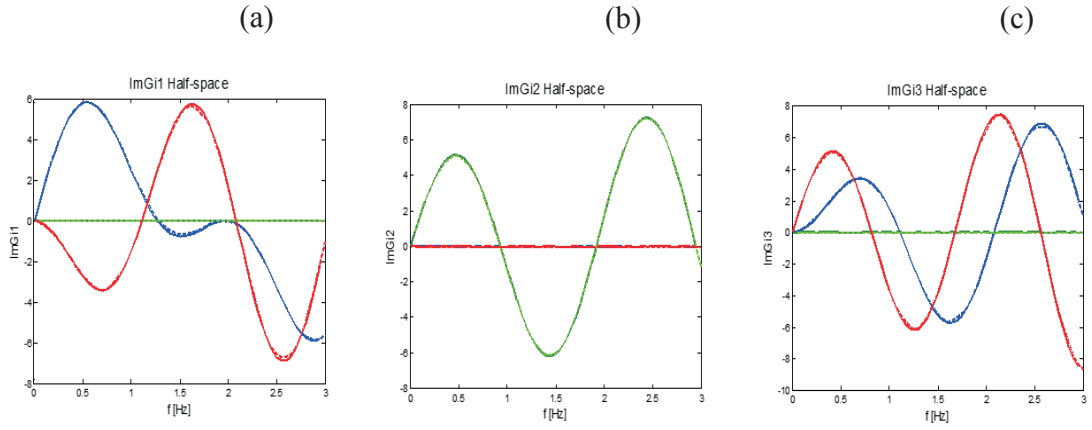

Figure 4. Imaginary part of Green functions G_{ij} for source and receiver at the free surface of half space. The source is at the origin while the receiver is at (1, 0, 0). Results in blue, green and red

correspond to *i*=1, 2, and 3, respectively. Panels (a), (b), and (c) represent *j*=1, 2, and 3 for horizontal (1 and 2) and vertical (3) loads. Results of correlations are depicted with continuous lines while the ones obtained with integral representations are given with dashed lines.

A natural extension of this idea for a layered half-space requires a description of surface waves within the set equipartitioned waves. Perton and Sanchez-Sesma (2015) present as an illustration the 2D case of a layer over a half-space for anti-plane SH excitation. In this case the density of states for SH waves for a narrow frequency band $d\omega$ is given by

$$dN_{SH} = \frac{\omega}{2\pi\beta^2} d\omega. \tag{12}$$

The energy density per unit area is $\xi = q \times dN_{SH} = q \frac{\omega}{2\pi\beta^2} d\omega$. Therefore, the constant q is

$$q = \frac{2\pi\xi\beta^2}{\omega \times d\omega}. \tag{13}$$

As the number of states for Love waves at the mode *m per unit length* is

$$N_{L_m} = \frac{\omega}{\pi c_m(\omega)} = \frac{1}{\pi} k_m, \tag{14}$$

the density of states related to mode m in the frequency band $d\omega$ around frequency ω is

$$dN_{L_m} = \frac{1}{\pi} \frac{\partial k_m}{\partial \omega} d\omega = \frac{1}{\pi} \frac{1}{U_m} d\omega, \tag{15}$$

where U_m = group velocity of mode *m*, therefore the energy density of mode *m* per unit length is given by

$$\xi_{L_m} = q \times dN_{L_m} = \left(\frac{2\pi\xi\beta^2}{\omega \times d\omega} \right) \frac{1}{\pi} \frac{1}{U_m} d\omega = \frac{2\beta^2 \xi}{\omega U_m}. \tag{16}$$

The imaginary part of Green's function $\mathrm{Im}\, G_{22}(A,B,\omega)$ is depicted in Fig 5. The agreement of the equipartitioned cocktail with the exact solution is excellent.

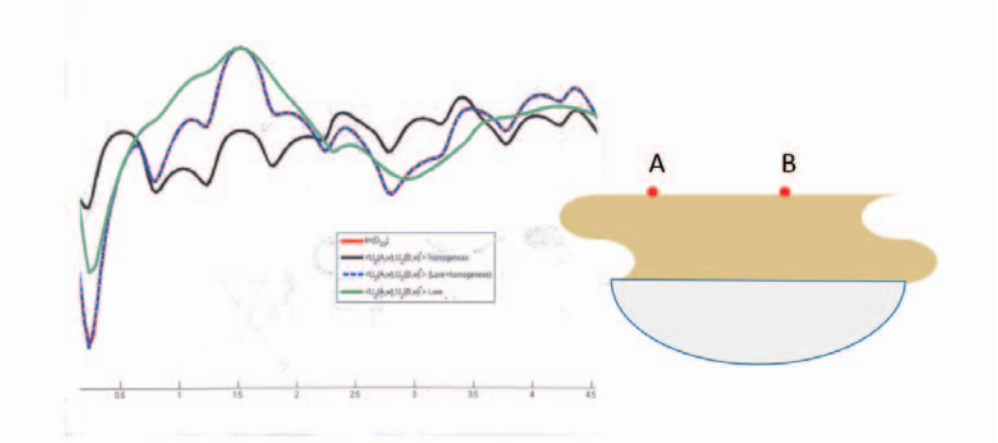

Figure 5. Results of the imaginary part of Green's function Im $G_{22}(A,B,\omega)$. Red line is the exact result while dotted line is the sum of equipartitioned cocktail. Black line corresponds to homogeneous waves while green one is for only surface modes.

H/V SPECTRAL RATIO AT z=0

The theory of diffuse fields relates the average energy densities to the Green's function. Then, *H/V* ratios (where H^2 and V^2 are the horizontal and vertical components of seismic energies) can be expressed as the ratio of the Green's tensor components for coinciding source and receiver. Assuming layered media without lateral heterogeneities, theoretical *H/V* ratios can be used for site characterization when comparing with the experimental counterpart obtained after appropriate noise normalization.
The energy densities provide the connection between field measurements and intrinsic properties of systems. For instance the spectra ratio H/V can be written in terms of measured energy densities by means of

$$[H/V](\omega) = \sqrt{\frac{E_1(\mathbf{x};\omega) + E_2(\mathbf{x};\omega)}{E_3(\mathbf{x};\omega)}} \,. \tag{17}$$

While the theory of diffuse fields implies

$$[H/V](\omega) = \sqrt{\frac{\mathrm{Im}[G_{11}(\mathbf{x},\mathbf{x};\omega)] + \mathrm{Im}[G_{22}(\mathbf{x},\mathbf{x};\omega)]}{\mathrm{Im}[G_{33}(\mathbf{x},\mathbf{x};\omega)]}} \,, \tag{18}$$

which is an intrinsic property of the system.

These result has been presented by Sánchez-Sesma et al (2011b) for layered media and 3D elastic fields. When body waves are the dominant part of the field Kawase et al. (2011) provide a useful formulation that is closely related to Clearbout's (1968).

Considering a single layer over a half space and the 3D formulation, the imaginary part of Green's functions G_{11} and G_{33} are depicted in Fig. 6.

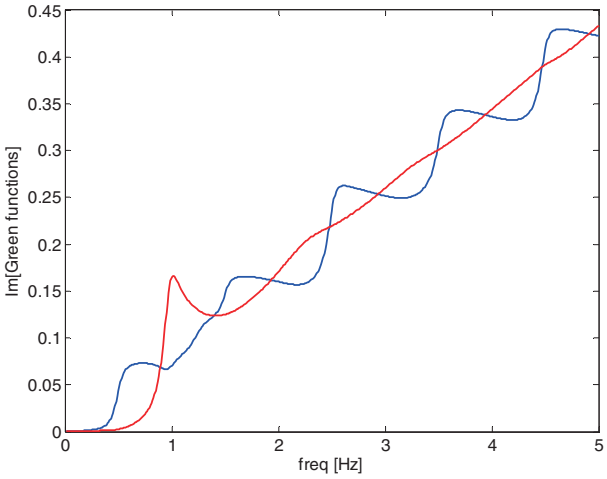

Figure 6 Imaginary part of Green's functions G_{11} and G_{33} for a layer over a half space. Blue line corresponds to horizontal response while red line represents vertical one.

Sánchez-Sesma *et al.* (2011b) did measurements in Texcoco, Mexico, a site within an ancient lake close to Mexico City. The results of computing Eq. 17 and the theoretical computations of Eq. 18 are depicted in Fig. 7.

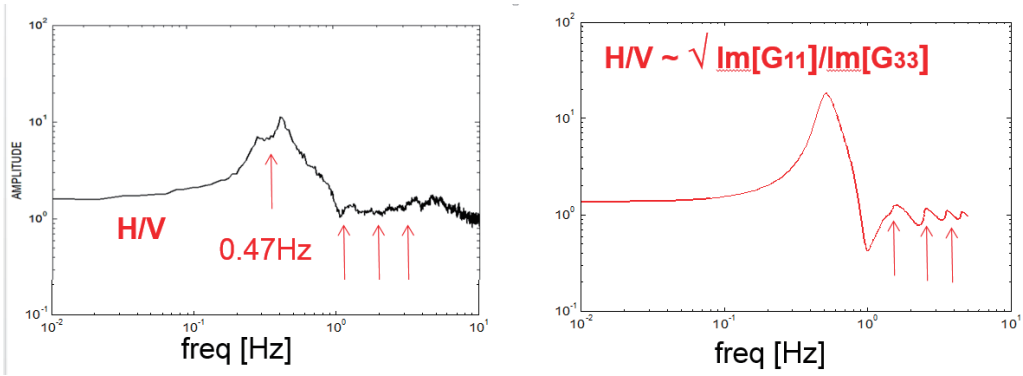

Figure 7 Spectral ratio H/V. Experimental (left) and theoretical results (right).

These results can be extended to measurements in depth (Lontsi *et al.* 2015) and for sites that take into account lateral irregularity (Matsushima *et al.* 2014).

The computation of theoretical results may be complicated. For layered medium they imply some integrals of the form:

$$\mathrm{Im}\left[G_{11}(r,0,0;0;\omega)\right] = \mathrm{Im}\left[\underbrace{\frac{i}{4\pi}\int_0^{+\infty} f_{SH}(k)\left[J_0(kr)+J_2(kr)\right]dk}_{SH} + \underbrace{\frac{i}{4\pi}\int_0^{+\infty} f^{H}_{PSV}(k)\left[J_0(kr)-J_2(kr)\right]dk}_{PSV}\right] \tag{19}$$

$$\mathrm{Im}\left[G_{33}(r,0,0;0;\omega)\right] = \mathrm{Im}\left[\frac{\mathrm{i}}{2\pi}\int_0^{+\infty} f_{PSV}^{V}(k) J_0(kr)\,dk\right]$$

where

$$f_{PSV}^{V}(k) = -\frac{[GN-LH]}{[NK-LM]},\quad f_{PSV}^{H}(k) = \frac{[RM-SK]}{[NK-LM]},\quad f_{SH}(k) = \frac{(J_L)_{12}-(J_L)_{22}}{(J_L)_{21}-(J_L)_{11}}$$

are the Harkrider's (1964) coefficients in terms of Haskell's (1956) propagators. The solution can also be achieved using the global matrix (Knopoff, 1964) as well (see Sánchez-Sesma et al. 2011b).

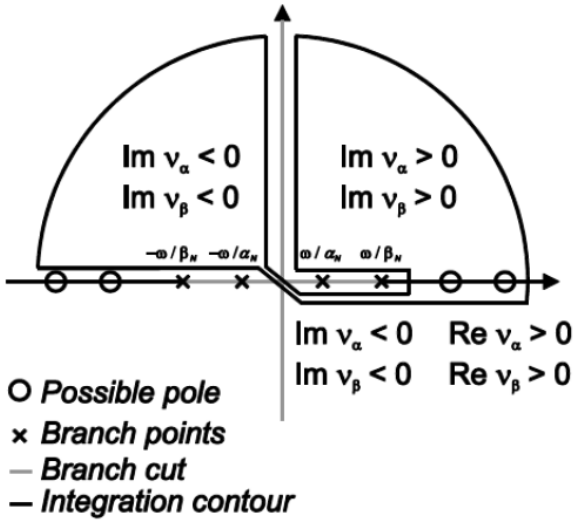

Figure 8. Integration contour in the complex k pane.
Branch points and poles on the real axis are sketched.

The numerical computations may require a very small discretization step and this could make inversion difficult. In order to speed of the process, the integrals for $r = 0$ can be made using contour integration in the complex k plane. García-Jerez *et al.* (2014) considered the contour depicted in Fig. 8. The branch points correspond to the zeroes of vertical wavenumbers:

$$\nu_{\alpha_N} = \sqrt{k^2 - (\omega/\alpha_N)^2} \qquad \nu_{\beta_N} = \sqrt{k^2 - (\omega/\beta_N)^2}$$

The result, in terms of Cauchy residue theory and some small numerical integrals can be written as (García-Jerez *et al.* 2013)

$$\mathrm{Im}[G_{11}^{PSV}(0;0;\omega)] = \mathrm{Im}[G_{22}^{PSV}(0;0;\omega)] = -\frac{1}{4}\sum_{m\in \mathrm{RAYLEIGH}} A_{Rm}\chi_m^2 + \frac{1}{4\pi}\int_0^{\omega/\beta_N} \mathrm{Re}\left[f_{PSV}^{H}(k)\right]_{4^{th}\,qu} dk$$

$$\mathrm{Im}[G_{11}^{SH}(0;0;\omega)] = \mathrm{Im}[G_{22}^{SH}(0;0;\omega)] = -\frac{1}{4}\sum_{m\in \mathrm{LOVE}} A_{Lm} + \frac{1}{4\pi}\int_0^{\omega/\beta_N} \mathrm{Re}\left[f_{SH}(k)\right]_{4^{th}\,qu} dk$$

$$\mathrm{Im}[G_{33}(0;0;\omega)] = -\frac{1}{2}\sum_{m\in \mathrm{RAYLEIGH}} A_{\mathrm{Rm}} + \frac{1}{2\pi}\int_0^{\omega/\beta_N} \mathrm{Re}\left[f_{PSV}^{V}(k)\right]_{4^{th}\,qu} dk\,,$$

where the residues are computed at the poles locations which correspond to Love and Rayleigh phase velocities given by the dispersion curves. The scheme of Fig. 9 presents the situation for the integrands of ImG_{11} and ImG_{33}.

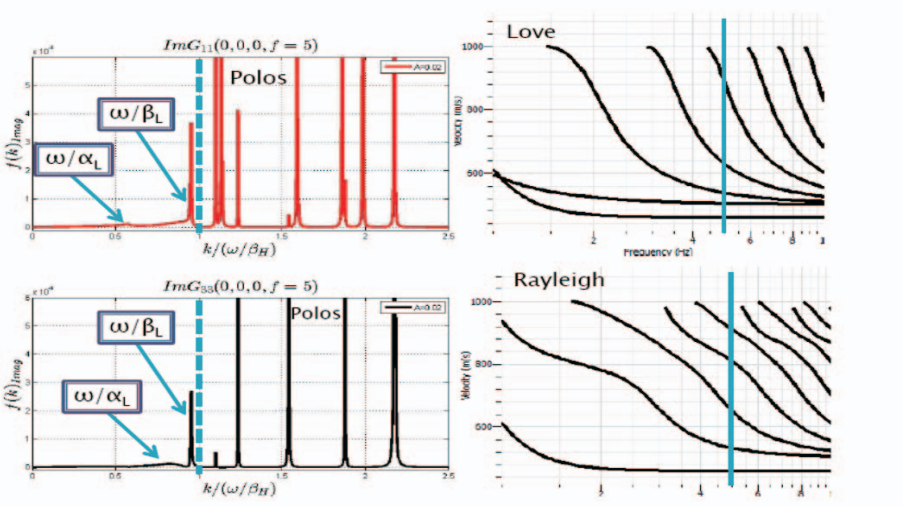

Figure 9. (left) Integrands of Im$G_{11}(0,0,k)$ and ImG_{33} $(0,0,k)$ for f=5Hz with small damping to enhance the poles in the k axis. (right) Dispersion curves for love and Rayleigh waves.

This analytical approach open the door to inversion. These approach for *H/V* has been presented by Piña-Flores (2015) in his MSc thesis and is the basis of a publication that will be presented elsewhere Piña et al. (2015).

Summarizing, in order to guarantee an effective inversion, the theoretical Green's functions must be efficiently computed. Computation is realized as the sum of an integral in the complex k plane over homogeneous plane waves and of the pole contributions due to Rayleigh and Love normal modes. These latter result from the application of the Cauchy residue theorem. The *H/V* ratios are not related linearly to the velocities and thicknesses. Thus, inversion is performed using "Simulated Annealing", a heuristic algorithm. The advantage of the method is that only one sensor is needed. When having more sensors, dispersion curves can also be retrieved from ambient noise measurements. Then, a joint inversion of both H/V and dispersion curves was implemented. The method allowed the significant reduction of local minima, and consequently a faster convergence to the solution. The joint inversion method has been validated using synthetic results (Piña-Flores, 2015).

H/V SPECTRAL RATIO AT $z \neq 0$

For sensors at depth (z≠0) the formulation of Eqs. 17 and 18 applies. Thus, it is possible to compute H/V for various depths. Lontsi et al. (2015) succeeded in the joint inversion for various sensors. Figs. 10 and 11 depict the inversion with only one sensor and the joint inversion with two sensors, one at the surface and other at depth (Lontsi et al. 2015).

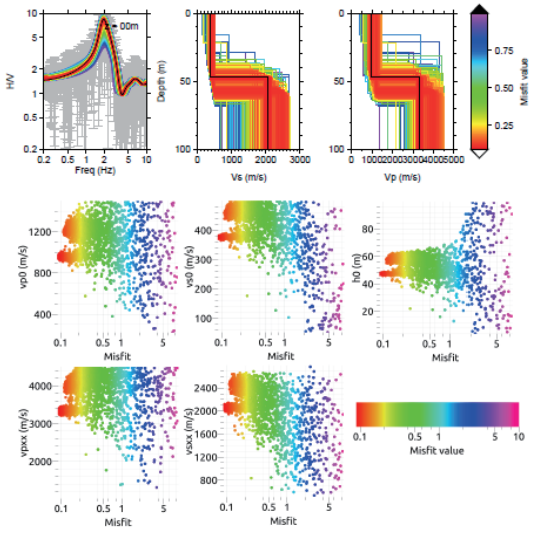

Figure 10. Full *H/V*(*f*,*z*=0) inversion. Synthetic result.

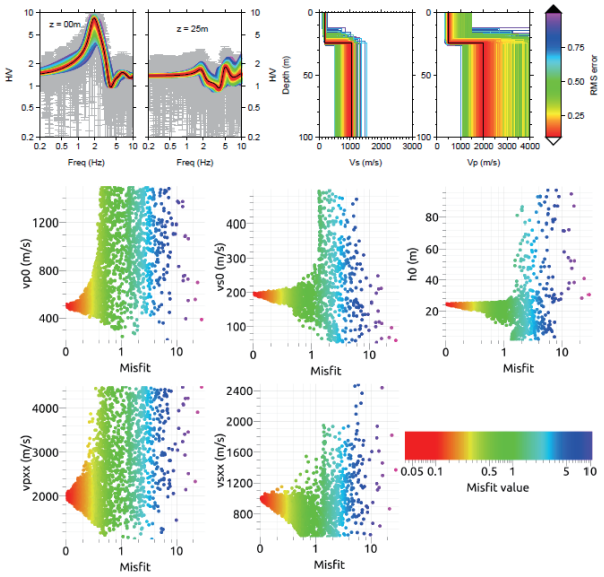

Figure 11. Full *H/V*(*f*,*z*=0) + *H/V*(*f*,*z*=25m) inversion. Synthetic result

These results shot the advantages of joint inversion. The improved definition of the inverted structure is the main by product.

CONCLUSIONS

We review briefly some applications of ambient seismic vibrations. It is clearly a wide subject. Following as a conducting thread the Principle of Equipartition of Energy and its implications in dynamic elasticity we link multiple scattering with the idea of diffuse fields in which the energy equilibrate to produce a diffuse field. The first experimental verification of these predictions is discussed. It was discussed that a random set of plane waves that fulfill the equipartition principle allows Green's function retrieval from correlations. A correlation type representation theorem is used as a tool to derive useful equations. Some emerging applications are discussed: The computation of Green's functions using equipartitioned cocktails of plane waves. The auto-correlations are related to directional energy densities and this leads to the deterministic partitions of energy and the interpretation of the noise H/V spectral ratio in terms of the Green's functions. This allows to deal with layered media and consider inversion from surface data and at depth. The effects of lateral heterogeneity can be studied from the same point of view. Without a doubt, these concepts will keep surprising us with new applications.

ACKNOWLEDGEMENTS

Thanks are given to U. Iturrarán-Viveros, H. Kawase, S. Matsushima, J C Molina-Villegas and M A Contreras-Zazueta for their constructive comments and suggestions, and to G. Sánchez and her team of the Unidad de Servicios de Información (USI) of the Institute of Engineering-UNAM for locating useful references. This work has been partially supported by AXA Research Fund and by DGAPA-UNAM under Project IN104712.

REFERENCES

Aki, K. (1957) Space and Time Spectra of Stationary Stochastic Waves, with Special Reference to Microtremors. Bull. Earthquake-Res. Inst. Tokyo, 35 . pp. 415-456.

Aki, K. and B. Chouet (1975). Origin of coda waves: Source, attenuation and scattering effects, J. Geophys. Res. 80, 3322-3342.

Campillo, M. (2006) Phase and Correlation in 'Random' Seismic Fields and the Reconstruction of the Green Function (2006) Pure and Applied Geophysics 163, 475-502.

Claerbout, J. F. (1968). Synthesis of a layered medium from its acoustic transmission response, Geophysics 33, 264–269.

Courtland, R. (2008), Harnessing the hum, Nature, 453, 146–148.

García-Jerez, A., F. Luzón, F. J. Sánchez-Sesma, E. Lunedei, D. Albarello, M. A. Santoyo, and J. Almendros (2013), Diffuse elastic wavefield within a simple crustal model. Some

consequences for low and high frequencies, *J. Geophys. Res. Solid Earth*, 118, doi:10.1002/2013JB010107

Gouédard, P., L. Stehly, F. Brenguier, M. Campillo, Y. Colin de Verdière, E. Larose, L. Margerin, P. Roux, F. J. Sanchez-Sesma, N. M. Shapiro and R. L. Weaver (2008). Cross-correlation of random fields: mathematical approach and applications, Geophysical Prospecting 56, 375-393.

Harkrider D.G. (1964) Surface waves in multi-layered elastic media. 1, Rayleigh and Love waves from buried sources in a multilayered elastic half-space, *Bull. Seism. Soc. Am. 54:627-680.*

Hennino, R., et. al. (2001). Observation of equipartition of seismic waves, Phys. Rev. Lett., 86, 3447–3450.

Kawase H, F J Sánchez-Sesma, and S. Matsushima (2011). The optimal use of horizontal-to-vertical (H/V) spectral ratios of earthquake motions for velocity structure inversions based on diffuse field theory for plane waves, Bull. Seismol. Soc. Am. 101, no. 5, 2001–2014, doi:10.1785/0120100263

Knopoff, L. (1964). A matrix method for elastic wave problems, Bull. seism. Soc. Am., 54, 431–438

Larose, E., et. al. (2006). Correlation of random wavefields: An interdisciplinary review, GEOPHYSICS, VOL. 71, NO. 4, SI11–SI21.

Lontsi A M, F J Sánchez-Sesma, J C Molina-Villegas, M. Ohrnberger and F. Kruger (2015). Full microtremor *H/V* (z, f) inversion for shallow subsurface characterization, in process.

Matsushima S, T Hirokawa, F De Martin, H Kawase, and F. J. Sánchez-Sesma (2014).The Effect of Lateral Heterogeneity on Horizontal-to-Vertical Spectral Ratio of Microtremors Inferred from Observation and Synthetics, *Bull. Seism. Soc. Am.* **104**, 381‑393,

Paul, A., M. Campillo, L. Margerin, E. Larose and A. Derode (2005) Empirical synthesis of time-asymmetrical Green function from the correlation of coda waves. Journal of Geophysical Research, 110, doi: 10.1039/2004JB003521.

Perton, M., F. J. Sánchez-Sesma, A. Rodríguez-Castellanos, M. Campillo, and R. L. Weaver (2009). Two perspectives on equipartition in diffuse elastic fields in three dimensions, J. Acoust. Soc. Am. 126 1125-1130, doi: 10.1121/1.3177262.

Piña-Flores J, (2015). *Cálculo e Inversión del cociente H/V a partir de ruido ambiental*, MSc Thesis, Posgrado en Ciencias de la Tierra, UNAM.

Piña-Flores J, M Perton, A García-Jerez, F J Sánchez-Sesma, and F Luzón (2015). Inversion of *H/V* ratio in layered media, Cargese, France.

Ryzhik, L. V., G. C. Papanicolau, and J. B. Keller (1996). Transport equations for elastic and other waves in random media, Wave Motion 24, 327-370.

Sánchez-Sesma, F. J., and M. Campillo (2006). Retrieval of the Green function from cross-correlation: The canonical elastic problem, Bull. Seism. Soc. Am. 96 1182-1191.

Sánchez-Sesma, F. J., J. A. Pérez-Ruiz, F. Luzón, M. Campillo, and A. Rodríguez-Castellanos (2008). Diffuse fields in dynamic elasticity, Wave Motion 45 641–654.

Sánchez-Sesma F J, Weaver R L, Kawase H, Matsushima S, Luzón, F and Campillo M (2011a), Energy Partitions among Elastic Waves for Dynamic Surface Loads in a Semi-Infinite Solid, Bulletin of the Seismological Society of America, Vol. 101. No. 4, pp. 1704-1709.

Sánchez-Sesma FJ, Rodríguez M, Iturrarán-Viveros, U, Luzón, F, Campillo M, Margerin L, García-Jerez A, Suárez M, Santoyo M, Rodríguez-Castellanos A (2011b). A Theory for microtremor H/V Spectral ratio: Application for a layered medium, *Geophysical Journal International* **186**, pp 221-225

Sato, H., and M. Fehler (1998). *Wave Propagation and Scattering in the Heterogeneous Earth*, Springer, New York.

Sato, H., M.C. Fehler, and T. Maeda (2012). *Seismic wave propagation and scattering the heterogeneous Earth*, (second edition) Springer editor

Shapiro, N. M., M. Campillo, L. Margerin, S. K. Singh, V. Kostoglodov and J. Pacheco (2000). The energy partitioning between P and S waves and the diffusive character of the seismic coda, Bull. Seism. Soc. Am. 90 655-665.

Snieder, R. (2002). Coda wave interferometry and the equilibration of energy in elastic media, Phys. Rev. E 66, 04615-1-8.

Snieder, R. and E. Larose, Extracting Earth's elastic wave response from noise measurements, Ann. Rev. Earth Planet. Sci., 41, 183-206, 2013

Stokes, G.G., 1849. On the dynamic theory of diffraction. Trans. Camb. Phil. Soc. 9, 1–62.

Wapenaar, K., D. Draganov, R. Snieder, X. Campman, and A. Verdel, Tutorial on seismic interferometry. Part 1: Basic principles and applications, Geophysics, 75, 75A195-75A209, 2010

Wapenaar, K., E. Slob, R. Snieder, and A. Curtis, Tutorial on seismic interferometry. Part 2: Underlying theory, Geophysics, 75, 75A211-75A227, 2010

Weaver, R.L. (1982). “On Diffuse Waves in Solid Media”, J. Acoust. Soc. Am., Vol. 71, pp. 1608-1609.

Weaver, R.L. (1985). “Diffuse Elastic Waves at a Free Surface”, J. Acoust. Soc. Am., Vol. 78, pp. 131–136.

1985年メキシコ地震の直後にメキシコ国立自治大学の工学研究所にて（後列左から，小林先生，ローゼンブルース教授，プリンス教授，ロムニッツ教授，瀬尾，前列左から，マリオ・オルダス，サンチェス・セスマ，翠川の各氏）